continued at room temperature for 0.8 h at which time ^{1}H NMR analysis showed 87% consumption of enol silane. The reaction mixture was diluted with pentane (10 mL) and extracted with saturated brine (8 mL). The aqueous layer was washed twice with pentane (10 mL). The combined organic layers were dried over Na_2SO_4 (1.5 g), filtered, and concentrated in vacuo. The pale yellow oil was purified by passing the mixture through a 1-in. plug of grade III basic alumina with hexane as eluant. A colorless oil, 86 mg (74% yield), was isolated. Anal. Calcd for $C_{17}H_{28}O_2Si$: C, 69.81; H, 9.64. Found: C, 69.86; H, 9.61. The extent of crossover was determined by ^{1}H NMR analysis. A sample of recovered TMS aldol **14** (25.4 mg, 0.087 mmol) was dissolved in $CDCl_3$ (0.5 mL), and the spectrum was run on a Bruker AM-500 spectrometer. To the solution was added two successive aliquots (10 and 15 μL) of 0.14 M TMS aldol-d_1 (4.1 mg in 0.10 mL $CDCl_3$). The first aliquot corresponded to addition of 1.6% deuterium-labeled aldol, while after the second addition 4.0% was present. Within the limit of detections, a conservative estimate of <3% crossover occurred during catalysis.

Acknowledgment. This research was supported by a research grant from the United States National Institutes of Health (GM 35699) and by a NIGMS Postdoctoral Fellowship to G.A.S. (GM 11265). We thank Drs. Thomas Tulip and Kenneth Feldman of Du Pont for informing us of their work on the preparation and characterization of rhodium enolates prior to publication.

Registry No. 1, 22710-50-5; **2**, 22481-17-0; **3**, 59175-43-8; **4**, 95070-47-6; **5**, 117775-76-5; **6**, 78904-15-1; **7**, 117800-21-2; **8**, 117800-22-3; **9**, 117800-23-4; (*E*)-**10**, 117800-24-5; (*Z*)-**10**, 117893-69-3; **11**, 117800-25-6; **12**, 117800-26-7; **13**, 117828-03-2; *syn*-**14**, 117775-79-8; *anti*-**14**, 117775-80-1; **15**, 66323-99-7; **16**, 13735-81-4; **16** (deuteriated), 117775-83-4; **21**, 61878-68-0; **22**, 73967-96-1; **23**, 117775-77-6; *syn*-**24**, 96816-44-3; *anti*-**24**, 96816-43-2; *syn*-**25**, 117775-78-7; *anti*-**25**, 117775-81-2; PhCOCH=CHPh, 94-41-7; μ-dichloro-tetracarbonyldirhodium(I), 14523-22-9; acetophenone, 98-86-2; propiophenone, 93-55-0; ethyl *tert*-butyl ketone, 564-04-5; ethyl mesityl ketone, 2040-15-5; (*E*)-1-mesityl-1-[(trimethylsilyl)oxy]-1-propene, 72658-15-2; (*Z*)-1-mesityl-1-[(trimethylsilyl)oxy]-1-propene, 72658-08-3; benzaldehyde, 100-52-7; *p*-tolualdehyde, 104-87-0; benzaldehyde-^{13}C, 10383-90-1; deuteriated (*Z*)-4,4-dimethyl-3-[(trimethylsilyl)oxy]-2-pentene, 117775-82-3.

Conversion of an Unsaturated Metallacycle into a Carbon-Rich *nido*-Metallacarborane. The BH Fragment as a Cluster Functional Group

Fung-E. Hong, Charles W. Eigenbrot, and Thomas P. Fehlner*

Contribution from the Department of Chemistry, University of Notre Dame, Notre Dame, Indiana 46556. *Received May 31, 1988*

Abstract: The reaction of the metallacycle Cp(PPh_3)$\overline{\mathrm{CoCPhCPhCPhC}}$Ph, **1**, with monoboranes containing at least one B–H bond provides a new route to the formation of a *nido*-metallacarborane, 3,4,5,6-tetraphenyl-1-(η^5-cyclopentadienyl)-3,4,5,6-tetracarba-1-cobalta-7-debor[D_{5h}-(151)-Δ^{10}*closo*]heptaborane(7), ($CpCoC_4Ph_4BH$) **2**, or, alternatively, a cobalt sandwich complex containing a borole ligand. Optimum yields of 30% are obtained by using a 10-fold excess of $BH_2Cl \cdot SMe_2$ as the source of B–H. The structure of **2** was determined by single-crystal X-ray diffraction methods, and the isomer isolated contains the cobalt atom in an apical position and the boron atom in a basal position. Crystals of **2** are orthorhombic with a = 14.956 (2) Å, b = 25.999 (2) Å, c = 12.933 (2) Å, V = 5028.8 Å^3, Z = 8, and space group *Pbca* (no. 61). The structure was solved by direct methods and refined to R = 0.037 and R_w = 0.040 for 3106 independent [$F_o \geq 2\sigma(F_o)$] reflections. The single B–H fragment in this heteroatom-rich cluster permits ready access to a variety of B-substituted compounds. The B–H bond is brominated under electrophilic conditions and alkylated with alkyllithium reagents. The B–Br bond is reduced with hydride, hydrolyzed to yield the B–OH derivative, and B-substituted with Grignard reagents. The B–OH functionality yields the B–OMe and B–$OSiMe_3$ derivatives. These reactions and the properties of **2** suggest that the boron atom can be usefully viewed as trivalent boron intramolecularly coordinated to the cobalt atom.

The use of heterocycles containing boron as ligands to transition metals is an established area of inorganic chemistry.[1-4] Compounds such as **2** (Figure 1) containing an η^5 borole ligand are already known.[1] This structure can also be viewed as a carbon-rich metallacarborane and, thus, is related to metallacarboranes containing a majority of boron atoms in the cage structure.[5] The usual synthetic approach to compounds like **2** is via the reaction of the free ligand or an appropriate precursor with a metal fragment source.[1-6] Likewise, for boron-rich compounds the approach is via the free carborane.[5] Alternatively there are a few examples of the insertion of an alkyne into a metallaborane.[7] A third route is the reaction of an organometallic complex with a source of borane. Insertion of boron in the ring of a π complex has led to borabenzene complexes.[1,3] This approach leads naturally to compounds containing isolated B–R fragments, i.e., carbon-rich metallacarboranes.

The utilization of the last route for the production of compounds containing B–H is unexplored.[8] A new route to these compounds would be interesting in a synthetic sense and would allow the reactions of a B–H fragment in a heteroatom cluster environment to be explored. Existing experimental information on a related

---

(1) For the most recent paper, see: Herberich, G. E.; Hessner, B.; Ohst, H.; Raap, I. A. *J. Organomet. Chem.* **1988**, *348*, 305.

(2) Siebert, W. *Adv. Organomet. Chem.* **1980**, *18*, 301.

(3) Herberich, G. E. In *Comprehensive Organometallic Chemistry*; Wilkinson, G., Stone, F. G. A., Abel, E. W., Eds.; Pergamon: Oxford, GB, 1982, Vol. 1, p 381.

(4) Siebert, W. In *Transition Metal Chemistry*; Müller, A., Diemann, E., Eds.; Verlag Chemie: Dearfield Beach, FL, 1981; p 157.

(5) Grimes, R. N. *Coordination Chem. Rev.* **1979**, *28*, 47. Grimes, R. N. In *Organometallic Reactions and Syntheses*; Becker, E. I., Tsutsui, M., Eds.; Plenum: New York, 1977; Vol. 6, p 63.

(6) Herberich, G. E.; Boveleth, W.; Hessner, B.; Hostalek, M.; Köffer, D. P. J.; Negele, M. *J. Organomet. Chem.* **1987**, *319*, 311. Herberich, G. E.; Boveleth, W.; Hessner, B.; Köffer, D. P. J.; Negele, M.; Saive, R. *J. Organomet. Chem.* **1986**, *308*, 153. Herberich, G. E.; Holger, O. *Chem. Ber.* **1985**, *118*, 4303.

(7) Weiss, R.; Bowser, J. R.; Grimes, R. N. *Inorg. Chem.* **1978**, *17*, 1522.

(8) Palladino, D. B.; Fehlner, T. P. *Organometallics* **1983**, *2*, 1692.

0002-7863/89/1511-0949$01.50/0 © 1989 American Chemical Society

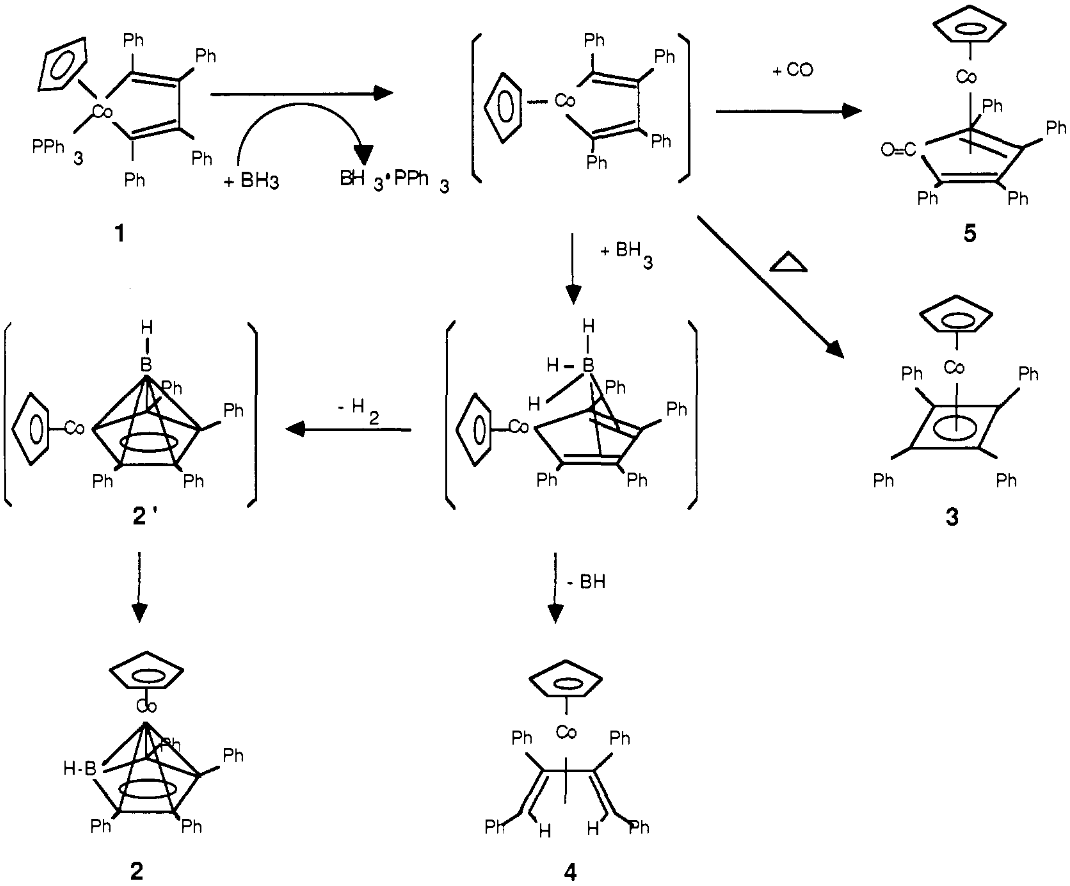

Figure 1. Schematic drawing of the proposed mechanism for the reaction of $\mathrm{Cp(PPh_3)\overline{CoCPhCPhCPhC}Ph}$ with BH_3·THF.

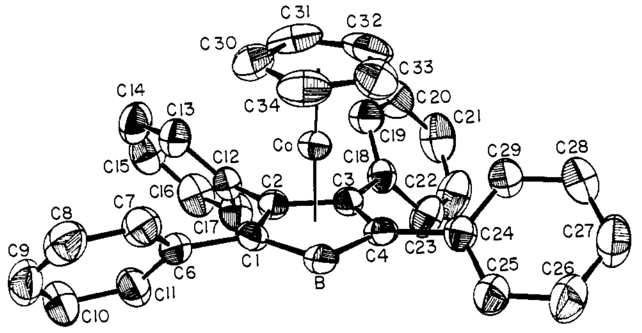

Figure 2. ORTEP drawing of the solid-state structure of **2**.

compound containing an isolated B–H fragment suggests useful reactivity.[9] Hence, the ability to place a B–H fragment, as opposed to a B–R fragment, into the cage may constitute a practical functionalization of the cage.

The metallacarborane **2** was chosen as the first target molecule because the B-phenyl derivative is known.[10] Hence, the reaction of the unsaturated metallacycle **1** with monoborane base adducts was examined. In doing so we anticipated that the borane would have a 2-fold role. First, action of the borane as a Lewis acid would trap the phosphine ligand necessarily released from **1** in the formation of **2** and, perhaps, facilitate its removal from **1** as well.[11] Second, addition of the borane to the double bonds of the metallacycle[12] followed by elimination of H_2 would lead to the desired product **2**. Both the metallacycle and borane are readily available; hence, one avoids the unsolved synthetic problem of making the parent borole.[13]

Results

Figure 1 presents a summary of the products containing a $(\eta^5\text{-}C_5H_5)Co$ fragment (CpCo) observed in the reaction of BH_3·THF with **1**. Besides the formation of BH_3·PPh_3 in high yield, the formation of H_2 during the reaction was established. With BH_3·THF the variety of products observed reflects a complex reaction pathway,[8] but variation in reaction conditions and B–H fragment source (see below) resulted in **2** as the predominant product containing a CpCo fragment. The previously known compounds **3**, **4**, and **5** were identified by their spectroscopic signatures, and **2** was characterized as described below.

Characterization of $CpCoC_4Ph_4BH$ (2). Compound **2** was isolated from the reaction mixture by thin-layer chromatography and characterized spectroscopically. The removal of the last traces of the borane·PPh_3 adduct from the product requires fractional crystallization of the product as a final purification step. The mass spectrum established the molecular formula of **2**, while the MS, IR, and ^{11}B NMR data showed the presence of a single B–H fragment. The ^1H NMR showed the presence of Ph and Cp in a 4:1 ratio. These data are consistent with the composition and structure shown for **2**.

As there was a possibility of producing an isomer of **2** with the isolobal CpCo and BH fragments interchanged (**2'**), the structure of the borane-containing product was determined in the solid state by a single-crystal X-ray diffraction study. The results are summarized in the ORTEP diagram shown in Figure 2. The observed structure is that of **2**, i.e., the CpCo fragment is in the apical position, and the B–H fragment is in a basal position of the CoC_4B nido cluster core. The parameters characterizing the cluster core are very similar to those obtained for the same core in a closely related compound.[14] Selected bond distances and angles are given in Table I. The B–C and C–C distances in the BC_4 ring are equal

---

[9] Ashe, A. J., III; Butler, W.; Standford, H. F. *J. Am. Chem. Soc.* **1979**, *101*, 7066.

[10] Herberich, G. E.; Buller, B.; Hessner, B.; Oschmann, W. *J. Organomet. Chem.* **1980**, *195*, 253.

[11] Hertz, R. K.; Goetze, R.; Shore, S. G. *Inorg. Chem.* **1979**, *18*, 2813.

[12] Brown, H. C. *Hydrocarbon*; Benjamin: New York, 1962.

[13] Eisch, J. J.; Galle, J. E.; Kozima, S. *J. Am. Chem. Soc.* **1986**, *108*, 379.

[14] Herberich, G. E.; Hessner, B.; Saive, R. *J. Organomet. Chem.* **1987**, *319*, 9.

Table I. Selected Interatomic Distances (Å) and Angles (deg) of **2**

Distances			
Co-C1	2.061 (3)	Co-C2	2.026 (3)
Co-C3	2.024 (3)	Co-C4	2.070 (3)
Co-C30	2.048 (3)	Co-C31	2.047 (3)
Co-C32	2.035 (4)	Co-C33	2.030 (3)
Co-C34	2.050 (3)	Co-B	2.147 (3)
C1-C2	1.448 (4)	C1-C6	1.478 (4)
C1-B	1.528 (4)	C2-C3	1.452 (4)
C2-C12	1.486 (4)	C3-C4	1.442 (4)
C3-C18	1.496 (4)	C4-C24	1.489 (4)
C4-B	1.526 (4)	C6-C7	1.398 (4)
C6-C11	1.389 (4)	C7-C8	1.379 (5)
C8-C9	1.369 (5)	C9-C10	1.377 (5)
C10-C11	1.391 (5)	C12-C13	1.394 (4)
C12-C17	1.395 (5)	C13-C14	1.383 (5)
C14-C15	1.374 (5)	C15-C16	1.382 (6)
C16-C17	1.386 (5)	C18-C19	1.385 (4)
C18-C23	1.385 (5)	C19-C20	1.382 (4)
C20-C21	1.378 (5)	C21-C22	1.366 (5)
C22-C23	1.403 (5)	C24-C25	1.393 (4)
C24-C29	1.398 (4)	C25-C26	1.389 (5)
C26-C27	1.379 (5)	C27-C28	1.380 (6)
C28-C29	1.385 (5)	C30-C31	1.414 (5)
C30-C34	1.408 (5)	C31-C32	1.376 (6)
C32-C33	1.403 (6)	C33-C34	1.403 (6)
Angles			
C2-C1-C6	122.8 (3)	C2-C1-B	108.4 (2)
C6-C1-B	128.6 (3)	C1-C2-C3	109.3 (2)
C1-C2-C12	125.8 (3)	C3-C2-C12	124.8 (3)
C2-C3-C4	109.4 (2)	C2-C3-C18	122.4 (3)
C4-C3-C18	128.1 (3)	C3-C4-C24	124.3 (3)
C3-C4-B	108.8 (3)	C24-C4-B	126.9 (3)
C1-C6-C7	122.2 (3)	C1-C6-C11	119.9 (3)
C7-C6-C11	117.8 (3)	C6-C7-C8	120.9 (3)
C7-C8-C9	120.5 (3)	C8-C9-C10	120.0 (3)
C9-C10-C11	119.7 (4)	C6-C11-C10	121.1 (3)
C2-C12-C13	121.8 (3)	C2-C12-C17	119.9 (3)
C13-C12-C17	118.2 (3)	C12-C13-C14	121.1 (3)
C13-C14-C15	120.0 (3)	C14-C15-C16	120.2 (3)
C15-C16-C17	120.2 (3)	C12-C17-C16	120.6 (3)
C3-C18-C19	122.5 (3)	C3-C18-C23	118.5 (3)
C19-C18-C23	118.9 (3)	C18-C19-C20	121.7 (4)
C19-C20-C21	119.1 (3)	C20-C21-C22	120.0 (3)
C21-C22-C23	121.2 (3)	C18-C23-C22	119.1 (3)
C4-C24-C25	118.2 (3)	C4-C24-C29	124.3 (3)
C25-C24-C29	117.6 (3)	C24-C25-C26	120.8 (4)
C25-C26-C27	120.7 (4)	C26-C27-C28	119.4 (3)
C27-C28-C29	120.1 (3)	C24-C29-C28	121.4 (3)
C31-C30-C34	107.6 (3)	C30-C31-C32	108.6 (4)
C31-C32-C33	108.1 (4)	C32-C33-C34	108.6 (4)
C30-C34-C33	107.1 (3)	C1-B-C4	104.1 (3)

to each other within experimental error, i.e., there is no geometrical evidence for localized C–C double bonds. The Co–B distance is significantly longer than those from cobalt to the C_4B ring carbons, hence, the metal does show a preference for the ring carbons over boron. The boron atom is slightly below the plane defined by the cage carbons [0.048 (3) Å] but within bonding distance of the cobalt atom [2.147 (3) Å]. The B–H hydrogen is out of the BC_4 plane toward cobalt such that the angle made at the boron atom by the center of the BC_4 ring and the B–H hydrogen is about 171°. The final B–H distance is 1.2 Å which is typical for terminal B–H bonds; the other atom–atom distances are also within normal ranges. The Cp and BC_4 rings are coplanar [dihedral angle 3.3 (15)°], and **2** can be viewed either as a sandwich complex with a borole ligand as one of the slices of bread[1-4] or as a metallacarborane isolobal with $C_4B_2H_6$.[4,5,15]

In reactions at higher temperatures another product containing boron was isolated which had the same molecular mass as **2** but different ^1H and ^{11}B NMR spectra. This is the compound we originally reported as having the structure of **2**, but it is, in fact, an isomer.[8] The structure of this isomer does not appear to be that of **2′**. As **2** is formed under lower temperature conditions we tried to convert **2** into **2′** by thermolysis. Our lack of success, combined with the fact that calculations (see below) indicated **2** as the thermodynamically most stable isomer, demonstrates that the isomer must have a significantly different, albeit unknown, structure from that of **2** or **2′**.

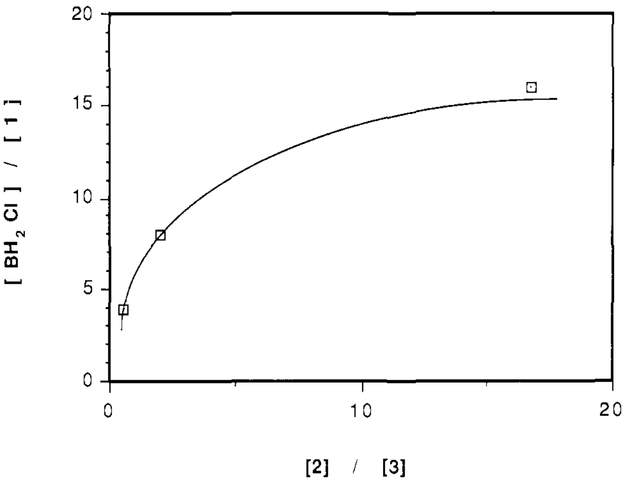

Figure 3. Plot of the ratio of $BH_2Cl·SMe_2$ to $Cp(PPh_3)CoCPhCPhCPhCPh$ (**1**) vs the ratio of $CpCoC_4Ph_4BH$ (**2**) to $CpCoC_4Ph_4$ (**3**).

Optimization of Yield and Selectivity. The initial yields of **2** using $BH_3·THF$ were low, and the product mixture contained substantial amounts of **3** and **4** (Figure 1). The presence of compound **4** was particularly annoying as it had an R_f value differing only slightly from that of **2** under optimum conditions. Pure samples of **2** could be obtained but only in small yields and with great effort. Hence, we spent some time investigating the source of these two particular byproducts in order to minimize their production.

The overall reaction was very slow at temperatures below 50 °C, and at temperatures above 90 °C **3** was the predominant product containing the CpCo fragment. The major pyrolysis product of **1** in the absence of borane[16] is **3** demonstrating loss of phosphine followed by an intramolecular rearrangement. Reaction of **1** with other Lewis bases also follows a dissociative pathway. For example, in the reaction of the tetramethyl derivative of **1** with alkynes, Bergman et al. found that dissociation of PPh_3 preceded reaction with an alkyne.[17] The rate of decomposition of **1** as a function of temperature is not appreciably changed in the presence of borane, hence, the loss of PPh_3 is probably still the slow step in the reaction. Consequently **3** results from intramolecular rearrangement of a 16-electron intermediate (Figure 1) with or without borane present in the reaction system.[16]

To test this conclusion, the reaction of **1** with 1–3 atm of CO with or without borane was investigated. The presence of CO leads to the suppression of **3** (and **4**) and the formation of **5** as the single major product containing CpCo.[18] The yield of **5** increases with increasing CO pressure, i.e., the addition of a trapping agent introduces a bimolecular reaction channel that competes effectively with the unimolecular reaction to produce **3**. In addition CO is a more effective trap for the intermediate than is borane.

In the absence of CO increasing amounts of **3** correlate with decreasing yields of **2** suggesting competitive pathways. As the reaction of the intermediate with borane must also be bimolecular, high levels of borane should promote product **2** relative to **3**. The data in Figure 3 substantiate this hypothesis where is is shown

---

(15) Groszek, E.; Leach, J. B.; Wong, G. R. F.; Ungermann, C.; Onak, T. *Inorg. Chem.* **1971**, *10*, 2770.

(16) Yamazaki, H.; Wakatsui, Y. *J. Organomet. Chem.* **1977**, *139*, 157.

(17) McAlister, D. R.; Bercaw, J. E.; Bergman, R. G. *J. Am. Chem. Soc.* **1977**, *99*, 1666.

(18) Nicholas, K. M.; Nestle, M. O.; Seyferth, D. In *Transition Metal Organometallics in Organic Synthesis*; Alper, H., Ed.; Academic Press: New York, 1978; Vol. 2.

that high levels of borane suppress the formation of **3** and result in higher absolute yields of **2**.

Presumably **4** is produced by a reduction of the intermediate by some source of hydrogen. Dihydrogen at 3 atm pressure did not increase the yield of **4**, and solvents, including THF, were eliminated as sources of the hydrogen. This left BH_3 itself as the source of hydrogen with the implication that after addition of BH_3 to the intermediate, B–H fragment loss is competitive with H_2 elimination. This is consistent with the facts that **4** is not suppressed by high levels of $BH_3{\cdot}THF$, and loss of B–H fragments in the reactions of polyhedral boranes and heteroboranes is well known.[19] Hence, we attempted to change the branching ratio by using substituted boranes. On investigating the effect of using $BH_2Cl{\cdot}SMe_2$ and $BHCl_2{\cdot}SMe_2$ as alternate B–H sources, we found total suppression of **4** and enhanced yields of the desired product **2**. Further, under these conditions there was no evidence for the formation of the B-chloro derivative of **2** and, indeed, reaction of **1** with $BCl_3{\cdot}SMe_2$ gave no product of the type sought here. The optimum yields are 30% (NMR) and 20% (isolated) using $BH_2Cl{\cdot}SMe_2$:**1** in a 10:1 ratio. Using other borane sources and similar reaction conditions, NMR yields are as follows: $BH_3{\cdot}THF$, 12%; $BH_3{\cdot}SMe_2$, 6%; $BHCl_2{\cdot}SMe_2$, 21%; $BCl_3{\cdot}SMe_2$, 0%; and $BH_3{\cdot}py$, 0%. These data indicate a dependence of yield on the base bound to borane. A weakly bound ligand on the borane promotes the formation of **2**.

Mechanism. Some aspects of the reaction mechanism whereby **2** is produced are revealed by the experiments above. Further clues come from analogous reactions reported in the literature. The reaction of **1** with $Fe_2(CO)_9$ leads to the formation of $CpCo(CO)_3FeC_4R_4$, the isolobal analogue of **2**, and a similar mechanism is suggested.[20] The intermediate formed by loss of phosphine (Figure 1) is a presumed intermediate in cobalt-mediated [2 + 2 + 2] reactions.[21] As the highest occupied molecular orbital (HOMO) of the 16-electron intermediate is associated with the C–C double bonds in the metallacycle ring,[22] attack of the electrophilic iron carbonyl fragment or borane at a double bond is reasonable. One wonders then why ligand dissociation is necessary as the double bond should be as reactive in **1** as in the intermediate. Indeed ligand dissociation suggests the possibility of attack at the metal. Hence, the tetraethyl derivative of **1** was investigated. Reaction with $BH_3{\cdot}THF$ takes place at 22 °C and below to yield the tetraethyl derivative of **2** as well as a variety of other boron- and non-boron-containing products.[23] Apparently, the seven phenyl groups on **1** prevent facile attack by borane, and it is only when the steric congestion is lowered by the loss of PPh_3 that the electrophilic addition of borane takes place at an observable rate. To probe the importance of unsaturation in the metallacycle, the reaction of $(PPH_3)CpCoCH_2CH_2CH_2CH_2$ with $BH_3{\cdot}THF$ was examined.[23] No evidence for a cobaltacarborane was found. Although this is negative evidence, it is consistent with attack of the unsaturated ring in **1**.

The addition of BH_3 to either **1** or the intermediate formed by the loss of PPh_3 (Figure 1) would lead naturally to **2′**; however, only **2** has been identified. In the course of these studies, we investigated via quantum chemical calculations the relative stability of **2** and **2′** as well as the magnitude of the barrier separating them. We found that the most stable isomer contains the B–H fragment in the base (**2**), and the barrier to rearrangement is a small fraction of the energy difference between isomers.[24] These results suggested that even if the isomer with an apical B–H were formed, it would not be stable under the reaction conditions. While our experimental work was in progress, we learned of similar calculations which have now appeared.[25] As our work is in substantial agreement with that in the literature, the details will not be repeated here but can be found elsewhere.[24]

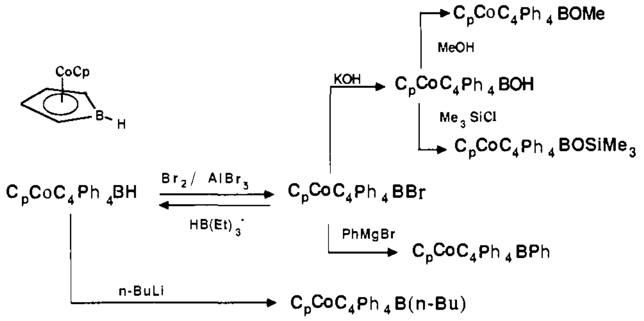

Figure 4. The reactions of $CpCoC_4Ph_4BX$, X = H, Br, OH.

The major products containing a CpCo fragment constitute between 30% and 50% of the product mixture. As shown by monitoring the reaction with ^1H NMR, between 40% and 60% of the sum of the intensities of the Cp signals are lost during the course of a typical reaction. This is attributed to direct attack of the borane on the Cp ring leading to the uncharacterized and insoluble black products. Direct insertion of a borane into a Cp ring has been observed by Herberich.[26] The less reactive boranes, e.g., $BH_2Cl{\cdot}SMe_2$, reduced the amount of precipitates thereby further increasing yield. However, increasing the borane/metallacycle ratio increased the amount of precipitate. Hence, the chosen borane/metallacycle ratio is a compromise between suppression of **3** and destruction of Cp. Significant improvement in the yield of **2** via this route requires the protection of the Cp ring. However, presumably for steric reasons, we were unable to synthesize the pentamethyl Cp derivative of **1**.

Reactivity of 2. We have explored the reactivity of the B–H fragment in **2** with respect to a number of standard organic derivatization procedures. A summary of the reactivity of **2** and some of the boron-substituted derivatives is given in Figure 4.

As halogenation of a B–H bond in polyhedral boranes is well known,[27] we examined the halogenation of **2** under electrophilic conditions. The C–H bonds of the phenyl substituents and, even though direct electrophilic halogenation of ferrocene is not known,[28] the C–H bonds of the Cp ligand are also potentially reactive sites. On the other hand, the boron of $CpCoC_4H_4BH$ has the most negative Mulliken population, and there is significant boron AO character in the HOMO.[24] Hence, the ground-state character of **2** suggests that substitution at boron should be favored over other possible sites.

The reaction of **2** with $AlBr_3$ and Br_2 proceeds smoothly when initiated at low temperatures producing a single product in about 70% isolated yield. Mass spectrometric analysis shows the replacement of a single hydrogen atom with a bromine atom. The ^1H NMR rules out substitution on the Cp ligand. The absence of a B–H stretch in the infrared spectrum and no observable B–H coupling combined with a positive shift in the boron resonance in the ^{11}B NMR demonstrates substitution at boron. The product is formulated as $CpCoC_4Ph_4BBr$.

Recently Ashe and co-workers[9] reported that bis(borabenzene)iron undergoes alkylation rather than lithiation when treated with butyllithium. Reaction of **2** with *n*-BuLi rapidly yields a single product in 55% isolated yield. Mass spectrometric analysis shows the replacement of a single hydrogen atom with a butyl group. The ^1H NMR rules out substitution on the Cp ligand and shows the presence of an *n*-butyl group. The absence of a B–H

---

[19] Onak, T. In *Boron Hydride Chemistry*; Muetterties, E. L., Ed.; Academic: New York, 1975; p 349.

[20] Yamazaki, H.; Yasufuku, K.; Wakatsuki, Y. *Organometallics* **1983**, *2*, 726. King, M.; Holt, E. M.; Radnia, P.; McKennis, J. S. *Organometallics* **1982**, *1*, 1718.

[21] Vollhardt, K. P. C. *Angew. Chem., Int. Ed. Engl.* **1984**, *23*, 539.

[22] Wakatsuki, Y.; Nomura, O.; Kitaura, K.; Morokuma, K.; Yamazaki, kH. *J. Am. Chem. Soc.* **1983**, *105*, 1907. Wakatsuki, Y.; Nomura, O.; Tone, H.; Yamazaki, H. *J. Chem. Soc., Perkin Trans. 2* **1980**, 1344.

[23] Feilong, J.; Fehlner, T. P. Unpublished work.

[24] Hong, F. E. Ph.D. Thesis, University of Notre Dame, Notre Dame, IN, 1988.

[25] Albright, T. P.; Lopez, J. P.; Silvestre, J. In *Quantum Chemistry: The Challenge of Transition Metals and Coordination Chemistry*; Veillard, A., Ed.; Reidel Publishing: New York, 1986; p 341.

[26] Herberich, G. E.; Greiss, G.; Heil, H. F. *Angew. Chem., Int. Ed. Engl.* **1970**, *9*, 805.

[27] Gaines, D. F. *Acc. Chem. Res.* **1973**, *6*, 416.

[28] *Gmelin Handbook of Inorganic Chemistry*, 8th ed.; New Supplement Series, Part A, Vol. 14, 1974; p 180.

stretch in the infrared spectrum and no observable B–H coupling combined with a positive shift in the boron resonance in the ^{11}B NMR demonstrates substitution at boron. The product is formulated as $CpCoC_4Ph_4B(n\text{-}Bu)$.

Reactions of $CpCoC_4Ph_4BBr$. As expected from the fact that $LiBEt_3H$ has been used to convert carbon-halogen bonds to C–H,[29] the reaction of $CpCoC_4Ph_4BBr$ with $LiBEt_3H$ results in the quantitative formation of **2**. The reactivity of $CpCoC_4Ph_4BBr$ with respect to Grignard reagents was tested by reaction with PhMgBr. The product produced in high yield was spectroscopically identical with the known compound $CpCoC_4Ph_4BPh$.[10]

The hydrolysis of $[Co(C_5H_5BBr)_2]^+$ yields an acidic solution containing $[Co(C_5H_5BOH)_2]^+$.[30] The basic hydrolysis of $CpCoC_4Ph_4BBr$ leads to two compounds containing boron. One formed in about 50% yield has a very low R_f value relative to $CpCoC_4Ph_4BBr$ or **2**. Mass spectrometric analysis shows the replacement of the bromine atom with a hydroxyl group. The ^{1}H NMR shows the presence of an O–H proton. The absence of a B–H stretch in the infrared spectrum and the presence of O–H and B–O bands confirms the presence of a B–OH moiety. The lack of B–H coupling combined with the value of the chemical shift in the ^{11}B NMR is consistent with the presence of B–OH in a tetrahedral environment. Hence, the product is formulated as $CpCoC_4Ph_4BOH$.

Reactions of $CpCoC_4Ph_4BOH$. The reaction of $CpCoC_4Ph_4BOH$ with MeOH leads, as expected, to $CpCoC_4Ph_4BOMe$ in high yield. Likewise the reactions of $CpCoC_4Ph_4BOH$ with $ClSiMe_3$ leads to $CpCoC_4Ph_4BOSiMe_3$.

Discussion

Although direct insertion of a borane into a coordinated cyclic ligand and the use of a borane to sequester a metal bound ligand have both been demonstrated separately,[11,26] this work illustrates a monoborane exhibiting both functions in converting an unsaturated metallacycle into a heteroatom-rich metallacarborane. Note that reaction of metallacycles containing a main group metal[31] or an early transition metal[32] leads to replacement of the metal and formation of the borole rather than addition and formation of a cluster or metal complex as observed here.

Although the mechanism sketched in Figure 1 is supported by the observations, it obviously is neither unique nor detailed. Exploratory studies on the reactions of metallacycles closely related to **1** show that relatively minor changes, e.g., substituents on the ring or on the phosphine, cause major changes in the observed mechanistic behavior.[17,23] For example, in closely related work we have shown that $CpCo(PPh_3)(C_2Ph_2)$, a metallacyclopropene, in the presence of $BH_3{\cdot}THF$ loses the organic ligand as well as the phosphine.[33] Again the borane serves in a dual role in effectively removing both the ligands from the reaction and in participating in the growth of clusters containing no carbon in the framework.

The incorporation of a B–H fragment into the cluster framework provides considerable synthetic flexibility. The B–H site in the coordinated borole is considerably more reactive than the C–H fragments of the Cp ligand or phenyl substituents. Like B–H fragments in most polyhedral boranes, facile electrophilic substitution by halogens is observed in conformity with the high calculated Mulliken population on boron. However, the B–H fragment also shows considerable reactivity with respect to nucleophilic displacement. Specifically, reaction of **2** with RLi is more reminiscent of reactions where the Lewis acidity of boron plays a key role. That is, with amine boranes,[34] borazine,[35] or cyclic dialkyl boron hydrides,[36] B–H bonds are converted to B–R bonds with LiR.[37]

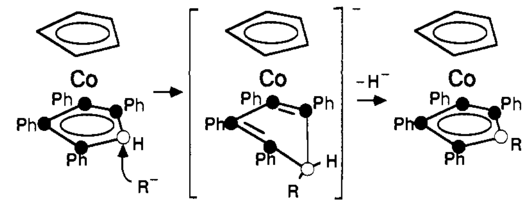

Figure 5. Proposed mechanism for the reaction of RLi with **2**.

Chart I

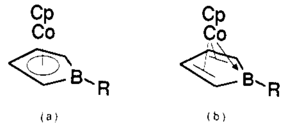

The boron in **2** is tetracoordinate but behaves as though it easily coordinates to a Lewis base. Hence, we propose the pathway shown in Figure 5 where coordination of the incoming nucleophile to the boron atom in **2** still leaves the cobalt atom with a formal 18-electron count. An analogous adduct is known for borabenzene complexes,[38] and adducts of free borole have been used for preparing complexes.[39] Loss of hydride then leads to the substituted product. In essence, the tetracoordinate boron in **2** is easily converted into a tricoordinate, and reactive, boron. Similar pathways have been proposed for closely related compounds.[40]

The B–Br fragment also serves as a useful functional group with, for example, Br^- being displaced by R^- or OH^-. The pathway envisioned is analogous to that shown in Figure 5. Production of the B–OH fragment permits access to additional chemistry. This has been demonstrated by the conversion of the B–OH fragment in **2** into B–OMe and $B\text{–}OSiMe_3$ fragments.

The reactivity of **2** is consistent with an alternative interpretation of the electronic structure (Chart Ib)[41] which emphasizes the fact that for the neutral ligand the electrons donated to cobalt formally come from the carbon atoms. Thus, there is a well-established relationship between the electronic properties of the cobalt atom and the nature of R, i.e., R groups that stabilize tricoordinate boron weaken the metal–boron donor–acceptor interaction.[41] The R group competes with cobalt for the out of plane boron orbital. A comparison of R = H and OH is pertinent. Compound **4** is deep red, and this absorption property is taken to be characteristic of the limit for very strong π donors on the boron atom of **2**. Compound **2** (R = H) is yellow (ν_{max} = 424 nM), while for R = OH the compound is deeply orange red (ν_{max} = 420, 520 nM), i.e., the π donor ability of the O–H fragment reduces the Co–B interaction creating an environment at cobalt more like that in **4**. This is confirmed by Fenske–Hall[42] calculations on

---

(29) Krishnamurthy, S.; Brown, H. C. *J. Org. Chem.* **1983**, *48*, 3085.

(30) Heil, H. F. Dissertation, Technische University, München, 1971.

(31) Ashe, A. J., III; Chan, W.-T. *J. Org. Chem.* **1979**, *44*, 1409. Ashe, A. J., III; Chan, W.-T.; Perozzi, E. *Tetrahedron Lett.* **1975**, 1083. See also earlier work by the following: Leusink, A. J.; Drenth, W.; Noltes, J. G.; van der Kerk, G. J. M. *Tetrahedron Lett.* **1967**, 1263. And a review: Corey, J. Y. *Adv. Organomet. Chem.* **1975**, *13*, 139.

(32) Fagan, P. J.; Burns, E. G.; Calabrese, J. C. *J. Am. Chem. Soc.* **1988**, *110*, 2979.

(33) Feilong, J.; Fehlner, T. P.; Rheingold, A. L. *J. Am. Chem. Soc.* **1987**, *109*, 1860. Feilong, J.; Fehlner, T. P.; Rheingold, A. L. *J. Chem. Soc., Chem. Commun.* **1987**, 1395. Feilong, J.; Fehlner, T. P.; Rheingold, A. L. *Angew. Chem., Int. Ed. Engl.* **1988**, *27*, 424. Feilong, J.; Fehlner, T. P.; Rheingold, A. L. *J. Organomet. Chem.* **1988**, *348*, C22.

(34) Köster, R. *Angew. Chem.* **1957**, *69*, 94.

(35) Powell, P.; Semelyen, J. A.; Blofeld, R. E.; Phillips, C. S. G. *J. Chem. Soc.* **1964**, 280.

(36) Brown, H. C.; Rogic, M. M. *J. Am. Chem. Soc.* **1969**, *91*, 4304.

(37) $B_{10}H_{14}$ also appears to undergo alkylation with LiR, but the site of reaction is different from that where electrophilic reactions are most favorable. Dunstan, I.; Williams, R. L.; Blay, N. J. *J. Chem. Soc.* **1964**, 280.

(38) Herberich, G. E.; Engelke, C.; Pahlmann, W. *Chem. Ber.* **1979**, *112*, 607.

(39) Herberich, G. E.; Hessner, B.; Negele, M.; Howard, J. A. K. *J. Organomet. Chem.* **1987**, *336*, 29.

(40) Herberich, G. E.; Ohst, H. *Adv. Organomet. Chem.* **1986**, *25*, 199.

(41) Siebert, W.; Full, R.; Edwin, J.; Kinberger, J.; Krüger, C. *J. Organomet. Chem.* **1977**, *131*, 1. Siebert, W.; Augustin, G.; Full, R.; Krüger, C.; Tsay, Y. *Angew. Chem., Int. Ed. Engl.* **1975**, *14*, 262. Siebert, W.; Full, R.; Edwin, J.; Kinberger, K.; Krüger, C. *J. Organomet. Chem.* **1977**, *131*, 1. Maddren, P. S.; Modinos, A.; Timms, P. L.; Woodward, P. *J. Chem. Soc., Dalton Trans.* **1975**, 1272. Howard, J. A. K.; Ken, E. W.; Woodward, P. *J. Chem. Soc., Dalton Trans.* **1975**, 2466. Herberich, G. E.; Hessner, B.; Beswethenick, S.; Howard, J. A. K.; Woodward, P. *J. Organomet. Chem.* **1980**, *192*, 421. Herberich, G. E.; Ohst, H.; Mayer, H. *Angew. Chem., Int. Ed. Engl.* **1984**, *23*, 969.

$CpCoC_4H_4BR$ (R = H, OH) using a fixed cluster framework as found in the structure of **2**. In going from R = H to OH, the HOMO–LUMO gap decreases which is consistent with the observed spectral changes. The Mulliken charge on the cobalt atom becomes less positive, and the Co–B overlap population decreases which is consistent with a smaller Co–B interaction in going to the B–OH derivative. In addition, in going from R = H to OH the C–C overlap populations of the C–C interactions corresponding to the formal double bonds of the classical structure (C1–C2 and C3–C4 in Figure 2) increase, while that of the formal single bond (C2–C3) decreases. This intramolecular competition between the cobalt atom and the R group for out-of-plane 2p orbital of the boron atom is consistent with the mechanism in Figure 4 where an intermolecular competition is proposed.

Conclusions

Monoboranes react with an unsaturated metallacycle to produce a metallacarborane. This approach provides a convenient route to a thermally stable metallacarborane with a single B–H in the cage skeleton. The presence of a B–H, as opposed to a B–R, fragment in the cage permits straightforward derivatization at the boron atom. Although the generality of the method has yet to be established, the availability of other types of metallacycles[43] or, indeed, other organometallic compounds with phosphine ligands, suggests considerable scope for application. In addition, the reaction of metallacycles such as **1** with other Lewis acids constitutes a potential route to cages containing main group elements other than boron.

Experimental Section

General Procedures. All reactions were carried out with standard Schlenk techniques.[44] Solvents were dried (toluene over anhydrous $MgSO_4$, THF over KOH pellets, hexane over molecular sieve), degassed, and distilled (from sodium–benzophenone ketyl) before use. The following reagents were used as received unless otherwise noted: BH_3·THF (1 M), BH_3·py (1 M), BH_3·SMe_2 (1 M), $BHCl_2$·SMe_2 (9 M), BH_2Cl·SMe_2 (9 M), BCl_3·SMe_2, C_4H_9Li (1.6 M in hexanes), PhMgBr·Et_2O (3 M), $HBEt_3Li$ (1 M in THF), Br_2, PPh_3, PhCCPh, $(CH_3)_3SiCl$ (Aldrich); $CoCl_2$·$6H_2O$, $AlCl_3$, Al(s), KOH (Fisher); $Fe(CO)_5$ (distilled under vacuum), NaCp (1.9 M in THF) (Alfa); H_2, CO (Linde). TLC plates (1B2-F silica gel, J. T. Baker) were used for following reaction progress. CTLC plates were prepared with 45 g of Merck silica gel 60-PF_{254} and 90 mL of H_2O for 1-mm plates and 60 g of silica gel and 120 mL of H_2O for 2-mm plates. Columns were prepared with Fisher 60–200 mesh silica gel.

Routine ^1H NMR spectra were obtained on a Magnachem A-200 FT spectrometer, and ^1H and ^{11}B NMR spectra were obtained on a Nicolet NB 300 FT spectrometer. Mass spectra were obtained on AEI-MS 9, DuPont DP-1, or Finnigan MAT 8450 mass spectrometers. IR spectra were recorded on Perkin Elmer 454, 420, or 983 spectrometers. UV–vis spectra were obtained on a Varian DMS-100 spectrometer. A Carle Model 311 gas chromatograph with molecular sieve and porapak columns in series and argon as a carrier gas was used to qualitatively identify evolved H_2. Elemental analyses were by Oneida Research Services. Chemical shifts are reported as follows: ^1H, residual signal of C_6D_6 δ 7.25; ^{11}B, external reference $B_3H_8NMe_4$ δ –29.7.

The synthesis of Cp(PPh_3)CoCPhCPhCPhCPh was patterned after procedures in the literature.[16]

Fenske–Hall calculations[42] were carried out as described previously.[45] For the results discussed herein, an idealized geometry derived from the solid-state structure of **2** with H replacing Ph was used independently of the substituent on boron.

Reaction of Cp(PPh_3)$\overline{\text{CoCPhCPhCPhC}}$Ph and BH_3·THF. Cp(PPh_3)CoC_4Ph_4 (2.1 g, 2.83 mmol) was placed in a 100-mL Schlenk flask with 30 mL of toluene. Four equivalents of BH_3·THF were slowly added to the solution at room temperature. The solution was stirred at 75 °C for 4 h. Analysis of the head gases showed the presence of significant amounts of H_2. After the reaction, a short silica gel column was used to separate the products from the black precipitate. The black residue, which stayed at the origin of the column, was not characterized. The products were separated from the reaction mixture by using repetitive centrifugal thin-layer chromatography (CTLC) with first hexane and then toluene. The first band (yellow) eluting with toluene in the initial separation was identified as $CpCoC_4Ph_4$ (**3**), a known compound.[16] The third band (colorless) was BH_3·PPh_3. The second band (orange) contained three compounds and was subjected to further CTLC. Three bands were isolated in the second separation. The first band (red) was characterized as a known compound, $CpCoC_4Ph_4H_2$ (**4**).[20] The second band (yellow) was a boron-containing compound $CpCoC_4Ph_4BH$ (**2**). The identity of the third band (yellow) is unknown. These constitute the optimum conditions for the formation of **2** with BH_3·THF. Yield of **2** is 12% in the mixture. It is less than 5% after separation and purification: ^1H NMR (C_6D_6, 25 °C) δ 7.0–7.8 (m, 20 H, Ph), δ 4.53 (s, 5 H, Cp); ^{11}B NMR ($CD_3C(O)CD_3$, 25 °C) δ 11, FWHM = 530 Hz, FWHM{^1H} = 400 Hz; MS, P^+ = *m/e* 492.125 (calcd 492.146), $P - 1^+ = 0.23$, $P^+ = 1.0$, $P + 1^+ = 0.35$, $P + 2^+ = 0.063$; IR (CsF, toluene) ν (BH) 2520 cm^{-1}, ν(Cp) 1069, 1056 cm^{-1}; UV–vis (toluene) 424 nM, sh. Elemental anal. Calcd for $C_{33}H_{26}Co_1B_1$: C, 80.51; H, 5.32. Found: C, 79.32; H, 5.03.

Reaction of Cp(PPh_3)$\overline{\text{CoCPhCPhCPhC}}$Ph and BH_2Cl·SMe_2. Cp(PPh_3)CoC_4Ph_4 (2.65 g, 3.57 mmol) was placed in a 250-mL Schlenk tube with 50 mL of toluene. BH_2Cl·SMe_2 (4 mL, 9 M, 35 mmol) was slowly added to the above solution at room temperature and was stirred for 4 h at 75 °C. After the reaction was complete, the solvent was pumped out completely under vacuum. Toluene (30 mL) was added to the residue, and a short silica gel column was used to separate the products from the green and brown precipitate. The crude mixture, containing 30% $CpCoC_4Ph_4BH$ (**2**) by NMR, was separated by CTLC. A minor yellow band eluted first with toluene and was identified as $CpCoC_4Ph_4$. The major yellow-orange band was collected, concentrated, and stored in a freezer overnight. The orange precipitate that formed was identified as pure **2**. The isolated yield of this compound is 17%. The mother liquor contained **2** plus a small amount of $CpCoC_4Ph_4$ and PPh_3·BH_3.

Reaction of Cp(PPh_3)$\overline{\text{CoCPhCPhCPhC}}$Ph with Other Borane Sources. A variety of other borane sources were investigated by using procedures very similar to those described above for BH_3·THF and BH_2Cl·SMe_2. After reaction, a short silica gel column was used to filter the solution, and a ^1H NMR of the reaction mixture with an internal standard was recorded. The yields of **2** were as follows: BH_3·SMe_2, 6%; $BHCl_2$·SMe_2, 21%; BH_3·py, 0%; BCl_3·SMe_2, 0%.

Reaction of Cp(PPh_3)$\overline{\text{CoCPhCPhCPhC}}$Ph with CO and without Borane. The pyrolysis of **1** with CO produces $CpCoC_4Ph_4CO$ (**5**).[18] A solution of **1** in toluene was split between two Schlenk flasks and each charged with 1 atm of CO. One equivalent of BH_3·THF was added to one of the flasks and both were heated in an oil bath at 65 °C for 4.5 h with stirring. The ^1H NMR spectra of the starting material and products were recorded with an internal standard. Only starting material (≈20% conversion, 96% mass balance based on the Cp resonances) and **5** (20%) were observed after reaction without borane. In the presence of borane starting material (≈40% conversion, 65% mass balance based on the Cp resonances), **4** (2%) and **5** (4%) were observed as products. The experiment was repeated at 75 °C with similar results except that the yield of **5** was higher (78%) and a small amount of **3** (3%) was observed. Similar results were observed at 75 °C with 1 and 3 atm of CO except that the yield of **5** improved at the higher CO pressure and that of **3** was suppressed. Compound **2** was not observed in the presence of CO.

Reaction of Cp(PPh_3)$\overline{\text{CoCPhCPhCPhC}}$Ph with H_2. A solution of **1** in toluene was split between two Schlenk flasks, and 1 equiv of BH_3·THF was added to each. One of the flasks had a N_2 atmosphere, while the other was charged with 3 atm of H_2. Both were heated in an oil bath at 75 °C for 4.5 h with stirring. The ^1H NMR spectra of the products were recorded with an internal standard. There was little difference in the product distribution.

Properties of CpCo(C_4Ph_4BH). The decomposition of **2** in toluene in air at room temperature had a half-life of 2 days. **2** reacts slowly in contact with H_2O in toluene/THF and after a period of several days a small amount of green precipitate is observed. No reaction of **2** in MeOH was observed by ^{1}NMR over a period of several days demonstrating little hydridic reactivity. A sample of **2** was sealed in a glass tube under vacuum and heated to 400 °C for an hour. The proton spectrum after heating showed that a significant amount of **2** survived, but no new signals were observed in the Cp region of the ^1H NMR.

Electrophilic Substitution of CpCo(C_4Ph_4BH). $CpCoC_4Ph_4BH$ (0.147 g, 0.3 mmol) was placed in a 50-mL flask with 10 mL of toluene. Aluminum powder (0.3 mmol) was placed in another 50-mL flask with 4 mL

---

[42] Hall, M. B.; Fenske, R. F. *Inorg. Chem.* **1972**, *11*, 768. Hall, M. B. Ph.D. Thesis, University of Wisconsin, Madison, WI, 1971. Fenske, R. F. *Pure Appl. Chem.* **1971**, *27*, 61.

[43] Chappell, S. D.; Cole-Hamilton, D. J. *Polyhedron* **1982**, *1*, 739.

[44] Shriver, D. R. *Manipulation of Air Sensitive Compounds*; McGraw-Hill: New York, 1975; p 241.

[45] DeKock, R. L.; Wong, K. S.; Fehlner, T. P. *Inorg. Chem.* **1982**, *21*, 3203.

Table II. Summary of Crystal Data and Intensity Collection Parameters for **2**

formula	$CoC_{33}BH_{26}$
fw, amu	492.32
$F(000)$	2048
crystal dimensns	0.30 × 0.36 × 0.38 mm
ω width at half-height	0.15°
Mo K(α) radiation	$\lambda = 0.71073$ Å
temp, °C	21 +/− 1°
space group	*Pbca*
a, Å	14.956 (2)
b, Å	25.999 (2)
c, Å	12.933 (2)
V, Å^3	5028.8
Z	8
density (calcd), g/cm^3	1.300
density (obsd), g/cm^3	1.317
diffractometer	Enraf-Nonius CAD4
monochromator	graphite crystal, incident beam
scan type	$\theta/2\theta$
scan rate	1.37 − 412°/min (in ω)
scan width, deg	$0.6 + 0.350 \tan \theta$
maximum 2θ	54.9°
reflcns measd	12777 total, 5735 unique
corrections	Lorentz polarization linear decay (from 1.000 to 1.026 on *I*) reflcn averaging (agreement on $I = 2.7\%$)
solution	direct methods
hydrogen atoms	included as fixed contribution
refinement	full-matrix least-squares
minimization function	$\sum w(\lvert F_{o2}\rvert - \lvert F_{c2}\rvert)^2$
least-squares weights	$4F_o^2/\sigma^2(F_o)^2 = 1/\sigma^2(F_o)$
anomalous dispersion	all non-hydrogen atoms
reflcns included	3106 with $F_o^2 > 2.0\sigma(F_o^2)$
parameters refined	316
R	0.037
R_w	0.040
esd of obsd of unit weight	1.04
convergence, largest shift	$0.00\ \sigma$
high peak in final diff map	0.27(5) e$^-$/Å^3
low peak in final diff map	−0.29(5) e$^-$/Å^3

Table III. Positional Parameters

atom	*x*	*y*	*z*	*B*(A2)[a]
Co	0.20222 (2)	0.17992 (1)	0.72040 (3)	2.779 (6)
C1	0.3028 (2)	0.1502 (1)	0.8113 (2)	2.80 (5)
C2	0.2228 (2)	0.1189 (1)	0.8148 (2)	2.78 (6)
C3	0.2002 (2)	0.10224 (9)	0.7109 (2)	2.77 (5)
C4	0.2658 (2)	0.1219 (1)	0.6392 (2)	2.94 (6)
C6	0.3449 (2)	0.1720 (1)	0.9049 (2)	3.10 (6)
C7	0.3678 (2)	0.2239 (1)	0.9126 (3)	3.96 (7)
C8	0.4106 (2)	0.2427 (1)	0.9991 (3)	4.85 (8)
C9	0.4330 (2)	0.2105 (2)	1.0787 (3)	5.22 (9)
C10	0.4119 (2)	0.1590 (2)	1.0733 (3)	5.17 (9)
C11	0.3687 (2)	0.1398 (1)	0.9861 (3)	4.21 (7)
C12	0.1743 (2)	0.1029 (1)	0.9099 (2)	3.07 (6)
C13	0.1420 (2)	0.1388 (1)	0.9808 (3)	3.94 (7)
C14	0.0987 (2)	0.1233 (1)	1.0700 (3)	5.00 (9)
C15	0.0876 (3)	0.0718 (2)	1.0902 (3)	5.34 (9)
C16	0.1198 (2)	0.0355 (1)	1.0215 (3)	5.05 (8)
C17	0.1629 (2)	0.0509 (1)	0.9319 (3)	4.18 (7)
C18	0.1230 (2)	0.0674 (1)	0.6889 (2)	3.01 (6)
C19	0.0374 (2)	0.0774 (1)	0.7243 (3)	3.81 (7)
C20	−0.0326 (2)	0.0438 (1)	0.7063 (3)	4.71 (8)
C21	−0.0170 (3)	−0.0004 (1)	0.6505 (3)	5.75 (9)
C22	0.0672 (3)	−0.0112 (1)	0.6157 (3)	5.9 (1)
C23	0.1387 (2)	0.0224 (1)	0.6344 (3)	4.52 (8)
C24	0.2605 (2)	0.1157 (1)	0.5249 (2)	3.20 (6)
C25	0.3400 (2)	0.1095 (1)	0.4701 (3)	4.56 (8)
C26	0.3394 (3)	0.1043 (2)	0.3633 (3)	6.1 (1)
C27	0.2603 (3)	0.1065 (2)	0.3087 (3)	5.7 (1)
C28	0.1810 (2)	0.1134 (1)	0.3613 (3)	4.68 (8)
C29	0.1810 (2)	0.1172 (1)	0.4682 (3)	3.81 (7)
C30	0.1605 (2)	0.2487 (1)	0.7810 (3)	4.41 (7)
C31	0.0860 (2)	0.2181 (1)	0.7534 (3)	5.17 (9)
C32	0.0907 (2)	0.2075 (1)	0.6494 (3)	5.77 (9)
C33	0.1674 (3)	0.2315 (1)	0.6097 (3)	5.59 (9)
C34	0.2111 (2)	0.2572 (1)	0.6907 (3)	4.70 (8)
B	0.3361 (2)	0.1520 (1)	0.6996 (3)	3.07 (7)

[a] Anisotropically refined atoms are given in the form of the isotropic equivalent displacement parameter defined as $(^4/_3)*[a^2*B(1,1) + b^2*B(2,2) + c^2*B(3,3) + ab(\cos \gamma)*B(1,2) + ac(\cos \beta)*B(1,3) + bc(\cos \alpha)*B(2,3)]$.

of THF. About 0.034 mL (0.6 mmol) of Br_2 was added to the second flask. The solution in the second flask was stirred for 3 h before it was transferred to the first flask which was cooled to −78 °C. The reaction mixture was allowed to warm to room temperature, and stirring was continued for 30 h until all the $CpCoC_4Ph_4BH$ was consumed as shown by TLC. More of the $AlBr_3/Br_2$ mixture (total of 2 mmol) was added to the reaction mixture during the course of the reaction. The reaction mixture was filtered through a syringe fitted with a glass frit, the solvent was pumped out completely, and the residue was dried for 1 h under vacuum. About 20 mL of toluene and 10 mL of diethyl ether were added to the flask. The flask was shaken gently to dissolve all the solid. A yellow compound precipitated after the flask was stored in the freezer for 1 h. After removing the solution, the yellow precipitate was washed twice with hexanes and dried for 1 h under vacuum. The product decomposes on silica gel. The final yield of $CpCoC_4Ph_4B$-Br was 70%: ^1H NMR (C_6D_6, 25 °C) δ 6.6–7.7 (m, 20 H, Ph), δ 4.49 (s, 5 H, Cp); ^{11}B NMR ($CD_3C(O)CD_3$, 25 °C) δ 17; MS, $P^+ = m/e$ 572, $P - 3^+ = 0.22$, $P - 2^+ = 0.95$, $P - 1^+ = 0.54$, $P^+ = 1.0$, $P + 1^+ = 0.34$, $P + 2^+ = 0.07$ (calcd 0.22, 0.96, 0.55, 1.0, 0.34, 0.06).

Reaction of $CpCo(C_4Ph_4BBr)$ with PhMgBr. A solution of 0.034 mmol of $CpCoC_4Ph_4BBr$ plus 5 mL of Et_2O was placed in a 25-mL Schlenk flask and cooled to 0 °C. PhMgBr (0.3 mmol, 0.1 mL, 3 M) was syringed in, and the solution was refluxed for 4 h. A small funnel with a frit was used to separate a white precipitate from the orange solution. An orange solid precipitated out after the solution was concentrated. The yield of $CpCoC_4Ph_4B$-Ph is 53%: ^1H NMR (C_6D_6, 25 °C) δ 6.7–7.9 (m, 25 H, Ph), δ 4.52 (s, 5 H, Cp); ^1H NMR (CD_2Cl_2, 25 °C) δ 6.8~7.9 (m, 25 H, Ph), δ 4.83 (s, 5 H, Cp); ^{11}B NMR ($C_6D_5CD_3$, 25 °C) δ 16.5; MS, $P^+ = m/e$ 568.1775 (calcd 568.1772), $P - 1^+ = 0.22$, $P^+ = 1.0$, $P + 1^+ = 0.42$, $P + 2^+ = 0.087$.

Reaction of $CpCo(C_4Ph_4BH)$ with *n*-BuLi. $CpCoC_4Ph_4BH$ (0.13 mmol) was placed in a 25-mL round flask and dissolved in 4 mL of toluene. BuLi (0.32 mmol, 0.2 mL, 1.6 M) was syringed into the solution which was at 0 °C. The color changed from orange to greenish yellow immediately when BuLi was injected into the flask. The solution was stirred for 5 min and then by separated in CTLC by using toluene. The first band (orange) was collected. The yield of $CpCoC_4Ph_4B$-Bu is 55%: ^1H NMR (C_6D_6, 25 °C) δ 6.8–8.0 (m, 20 H, Ph), δ 4.55 (s, 5 H, Cp), δ 1.05 (t, 3 H, CH_3), δ 1.40 (m, 2 H, CH_2), δ 1.62 (m, 2 H, CH_2), δ 1.80 (t, 2 H, CH_2); ^{11}B NMR ($C_6H_5CH_3$, 25 °C) δ 19.5 ppm; MS, $P^+ = m/e$ 548.2085 (calcd 548.2085), $P - 1^+ = 0.24$, $P^+ = 1.0$, $P + 1^+ = 0.33$, $P + 2^+ = 0.10$.

Reaction of $CpCo(C_4Ph_4BBr)$ with KOH. A 20-mL Schlenk flask containing 0.026 mmol of $CpCoC_4Ph_4BBr$ and 6 mL of toluene was cooled to −78 °C, and 0.03 mmol of KOH powder was added. The solution was allowed to warm up to room temperature and was stirred overnight. About 3 more equiv of KOH were placed in the tube, and the solution was stirred for 2 more h till all the starting material was consumed. CTLC with toluene followed by CH_2Cl_2 was used to separate the products. The yellow band which eluted with CH_2Cl_2 was collected. The yield of $CpCo(C_4Ph_4B$-OH) is about 50%: ^1H NMR (C_6D_6, 25 °C) δ 6.8–8.0 (m, 20 H, Ph), δ 4.52 (s, 5 H, Cp), δ 3.30 (s, 1 H, OH); ^{11}B NMR ($C_6H_5CH_3$, 25 °C) δ 23 ppm; MS, $P^+ = m/e$ 508.1404 (calcd 508.1408), $P - 1^+ = 0.23$, $P^+ = 1.0$, $P + 1^+ = 0.35$, $P + 2^+ = 0.06$; IR (CsF, toluene) ν(O–H) 3625 cm^{-1}, ν(B–O) 1595 cm^{-1}; UV–vis (toluene) 420 sh, 520 nM.

Reaction of $CpCoC_4Ph_4B$-OH with MeOH and Me_3SiCl. An excess of MeOH was added to a Schlenk flask containing about 0.01 mmol of $CpCoC_4Ph_4B$-OH in toluene. After stirring at room temperature for 48 h, the product was separated from unreacted starting material with a short silica gel column by using toluene, and the orange band eluting first was collected. The yield of $CpCoC_4Ph_4B$-OMe was about 50% [^1H NMR (C_6D_6, 25 °C) δ 6.8–8.0 (m, 20 H, Ph), δ 4.67 (s, 5 H, Cp), δ 3.75 (s, 3 H, CH_3); MS, $P^+ = m/e$ 522.1568 (calcd 522.1565), $P - 1^+ = 0.23$, $P^+ = 1.0$, $P + 1^+ = 0.35$, $P + 2^+ = 0.07$]. A similar sample of $CpCoC_4Ph_4B$-OH was cooled to −78 °C before adding 0.1 mL of Me_3SiCl and 0.1 mL of Et_3N. After warming to room temperature, the mixture was stirred for 10 h monitoring the reaction progress by TLC. The first orange band eluting with toluene from a short silica gel column was collected. The yield of $CpCoC_4Ph_4B$-$OSiMe_3$ was about 50%: ^1H NMR (C_6D_6, 25 °C) δ 6.8–8.0 (m, 20 H, Ph), δ 4.61 (s, 5 H, Cp), δ 2.33 (s, 9 H, CH_3); MS, $P^+ = m/e$ 580.1803 (calcd 580.1804), $P = 1^+ = 0.22$, $P^+ = 1.0$, $P + 1^+ = 0.43$, $P + 2^+ = 0.12$, $P + 3^+ = 0.03$.

Crystal Structure of 2. An orange, regular parallelepiped crystal of **2** having approximate dimensions of 0.30 × 0.36 × 0.38 mm was mounted in a glass capillary in a random orientation. Cell constants and an orientation matrix for data collection were obtained from least-squares refinement, by using the setting angles of 25 reflections in the range 12° < |2Θ| < 15°, yielding the cell parameters given in Table II. From the systematic absences of *hk*0, *h* = 2*n*; *h*0*l*, *l* = 2n; 0*kl*, *k* = 2*n* and subsequent least-squares refinement, the space group was determined to be *Pbca* (no. 61). Moving-crystal moving-counter background counts were made by scanning an additional 25% above and below this range. Thus the ratio of peak counting time to background counting time was 2:1. The counter aperture was 3.0 mm wide by 4.0 mm high. The diameter of the incident beam collimator was 1.5 mm, and the crystal to detector distance was 21 cm.

A total of 12 777 reflections (+*h*,+*k*,+/−*l*) were collected, of which 5735 were unique and not systematically absent. As a check on crystal and electronic stability, four representative reflections were measured every 60 m of X-ray exposure. A total loss in intensity of 5.0% was observed and a linear decay correction was applied. The correction factors on *I* ranged from 1.000 to 1.026 with an average value of 1.011. Lorentz and polarization corrections were applied to the data. The linear absorption coefficient is 7.0 cm^{-1} for Mo K(α) radiation. ψ scans of five reflections with Θ between 4.45 and 14.66° showed small variations in intensity. No absorption correction was made, the largest error left untreated thereby being approximately 2% on *I*. Intensities of equivalent reflections were averaged. The agreement factors for the averaging of the 5269 observed and accepted reflections was 2.7% based on intensity and 2.4% based on F_o. (Eleven reflections were rejected from the averaging statistics because their intensities differed significantly from their average. This was due to large ratios of $I/\sigma I$.)

The structure was solved by direct methods by using the data up to $\sin \Theta/\chi = 0.478$ (0.4 of a copper sphere). Using 319 reflections (minimum E of 1.50) and 12 655 relationships, a total of 21 phase sets were produced. The cobalt ion was located from an E-map prepared from the phase set with probability statistics: absolute figure of merit = 1.32, residual = 14.45, and $\psi_0 = 2.291$. No other atoms were discerned in this E-map, but the cobalt position was confirmed by a Patterson map. The remaining atoms were located in succeeding difference Fourier syntheses. Hydrogen atom positions were calculated and then added to the structure factor calculations, but their positions were not refined. The position of the hydrogen atom bonding to the boron was taken from a persistent difference peak. The structure was refined in full-matrix least squares where the function minimized was $\sum w(|F_o| - |F_c|)^2$, and the weight *w* is defined as: $w = 4F_o^2/\sigma^2(F_o^2) = 1/\sigma^2(F_o)$. The standard deviation on intensities, $\sigma(F_o^2)$, is defined as $\sigma^2(F_o) = [S^{2*}(C + R^2B) + (pF_o^2)^2]/\mathrm{Lp}^2$, where *S* is the scan rate, *C* is the total integrated peak count, Lp is the Lorentz-polarization factor, and the parameter *p* is a factor introduced to downweight intense reflections. Here *p* was set to 0.040.

Scattering factors were taken from Cromer and Waber.[46] Anomalous dispersion effects were included in F_c;[47] the values for $\Delta f'$ and $\Delta f''$ were those of Cromer.[48] Only the 3106 reflections having intensities greater than 2.0 times their standard deviation were used in the refinements. The final cycle of refinement included 316 variable parameters and converged with unweighted and weighted agreement factors of $R_1 = \sum|F_o - F_c|/\sum|F_o| = 0.037$ and $R_2 = [\sum w(F_o - F_c)^2/\sum wF_o^2]^{0.5} = 0.040$. The standard deviation of an observation of unit weight was 1.04. There were no correlation coefficients greater than 0.50. The final difference Fourier map was judged to be featureless. Plots of $\sum w(|F_o| - |F_c|)^2$ vs $|F_o|$, reflection order in data collection, $\sin(\Theta)/\lambda$, and various classes of indices showed no unusual trends. Final positional parameters are given in Table III, and thermal parameters appear in the Supplementary Material.

Acknowledgment. We are grateful for the support of the National Science Foundation and the Petroleum Research Fund, administered by the American Chemical Society, as well as the contributions of D. B. Palladino and J. Feilong to early and related studies, respectively. The support of the DAAD and the hospitality of Prof. Dr. W. Siebert at Heidelberg where the seeds of these ideas were planted are also gratefully acknowledged. We thank Prof. T. A. Albright for information in advance of publication and appreciate the comments of a referee.

Supplementary Material Available: Listing of thermal parameters and hydrogen atom positions and the packing diagram (6 pages); listing of observed and calculated structure factor amplitudes (29 pages). Ordering information is given on any current masthead page.

---

(46) Cromer, D. T.; Waber, J. T. *International Tables for X-ray Crystallography*; The Kynoch Press; Birmingham, GB, Vol. IV, 1974; Table 2.2B.
(47) Ibers, J. A.; Hamilton, W. C. *Acta Crystallogr.* **1964**, *17*, 781.
(48) Cromer, D. T.; Waber, J. T. *International Tables for X-ray Crystallography*; The Kynoch Press: Birmingham, GB, Vol. IV, 1974; Table 2.3.1.

Rate Constants for the Reactions t-C_4H_9 + DX → i-C_4H_9D + X (X = Br, I), 295 < T (K) < 384: Heat of Formation of the *tert*-Butyl Radical

Wolfgang Müller-Markgraf, Michel J. Rossi,* and David M. Golden

Contribution from the Department of Chemical Kinetics, Chemical Physics Laboratory, SRI International, Menlo Park, California 94025. *Received May 23, 1988*

Abstract: Absolute values for the rate constants of the metathesis reactions of DX (X = Br, I) with *tert*-butyl, generated by 351-nm photolysis of 2,2′-azoisobutane, were determined in a low-pressure Knudsen cell reactor using the VLPΦ (very low pressure photolysis) technique. For X = Br, the values are $10^{-8}k$ (M^{-1} s^{-1}) = 0.9 and 2.3, and for X = I the values are 2.1 and 3.1 at 295 and 384 K. The latter are in good agreement with earlier measurements from this laboratory. The former values are lower by a factor of 50 compared to those recently reported at 295 K and fail to show the negative activation energy found in that work. Correcting by $\sqrt{2}$ for the primary isotope effect and combining with the rate constants for the reverse reactions lead to $\Delta H_f{}^\circ{}_{298}$(*tert*-butyl) (kcal mol^{-1}) = 9.2 ± 0.5 in both cases. First-order heterogeneous loss of *tert*-butyl radicals on the Teflon-coated surface employed is small (<2 s^{-1}).

The importance of knowledge of thermochemical data for *tert*-butyl radicals and other prototypical radicals (e.g., *i*-propyl, ethyl, and methyl) has been addressed by many authors in the past.[1-5] The persisting discrepancies between data derived from different types of kinetic studies, e.g., from iodination/bromination investigations[3,4,6-8]

$$\text{R-H} + \text{X} \leftrightarrow \text{HX} + \text{R} \qquad \text{X} = \text{Br, I}$$

---

(1) Russell, J. J.; Seetula, J. A.; Timonen, R. S.; Gutman, D.; Nava, D. J. *J. Am. Chem. Soc.* **1988**, *110*, 3084.
(2) Russell, J. J.; Seetula, J. A.; Gutman, D. *J. Am. Chem. Soc.* **1988**, *110*, 3092.
(3) Rossi, M. J.; Golden, D. M. *Int. J. Chem. Kinet.* **1983**, *15*, 1283.
(4) Rossi, M. J.; Golden, D. M. *Int. J. Chem. Kinet.* **1979**, *11*, 969.
(5) Choo, K. Y.; Beadle, P. C.; Piszkiewicz, L. W.; Golden, D. M. *Int. J. Chem. Kinet.* **1976**, *8*, 45.

0002-7863/89/1511-0956$01.50/0